Close and Return

Electrical properties of microvaristor composites

Dimitri CHARRIER, Xavier FESTAZ, Arnaud ALLAIS; Nexans Research Center, 29 rue Pré Gaudry, 69353 Lyon (France), dimitri.charrier@nexans.com, xavier.festaz@nexans.com, arnaud.allais@nexans.com
Guillaume ESCAMEZ; Institut Néel, 25 Rue des Martyrs, 38042 Grenoble (France)
guillaume.escamez@grenoble.cnrs.fr

ABSTRACT

In the development for cable systems, the accessories are usually identified as weak points due to complex electric field distributions. For an HVDC system, resistive field grading materials offer solutions to cope with DC and transient phenomena. However, their realization requires deeper understanding of electrical behaviors which are driven mainly by interfaces between materials constituting a composite, i.e., between filler particles, filler particles and the matrix, and inside the filler particles themselves. In this contribution, we present a methodology for measuring intrinsic physical properties of non-linear materials.

KEYWORDS

HVDC, varistor, composite, activation energy

I. INTRODUCTION

Zinc oxide is a widely studied electronic material for numerous applications [1], [2]. In particular, ZnO based varistors are commonly used in electrical power devices [3]. Additions (the major one is bismuth oxide; Bi_2O_3), and appropriate thermal treatment lead to a microstructrue with heterogeneous electronic properties of conducting ZnO grains and insulating grain boundaries [4]. Pure ZnO is known to be an electron donor (n doped) due to oxygen vacancies [5]. Grain boundaries decorated with Bi-rich phase are characterized by a different band gap and Fermi level. Thus the resulting ZnO//Bi-rich-phase//ZnO interface behaves as a diode junction [6]: electrons have to overcome the potential barrier at the interface, which is just the working principle of a diode.

Composites made of microvaristors distributed in an organic matrix, present reliable mechanical and electrical performances for power devices [7], [8]. Figure 1 schematically shows the microstructure of such a composite: particles are made of assembly of homogeneous ZnO grains separated by grain boundaries. Every grain boundary in a conduction path can be considered as a diode.

II. ELECTRICAL MODELING

At the interfaces acting as a diode, the electronic transport is described by the Shockley [9] equation (Eq. [1], [2]).

$$I_{diode} = I_S\left(\exp\left(\frac{eV}{kT}\right) - 1\right) \quad [1]$$

with

$$I_S = I_{0S}T^{3+\gamma/2}\exp\left(-\frac{E_g}{kT}\right) \quad [2]$$

where e is the elementary charge, V the applied potential, k the Boltzmann constant, T the temperature, I_{0S} the proportional factor, γ the injection efficiency and E_g the gap energy. For ideal diodes, $\gamma = 3$ [9]. In a varistor composite (VR) containing M in-parallel and N in-series connected identical diodes, the resulting current is:

$$I_{VR} = MI_S\left(\exp\left(\frac{eV}{NkT}\right) - 1\right) \quad [3]$$

Knowledge of intrinsic properties such as gap energy E_g or conduction path length helps in describing macroscopic behavior in complex distribution of temperature and electric field. Experimental data (IV curves) were fitted with the model expression that contains intrinsic properties.

III. EXPERIMENT

Sample preparation

One millimeter thick plates of composite material were prepared by adding microvaristor particles in a matrix of ethylene propylene diene monomer (EPDM) rubber followed by molding in a press. The volume ratio of microvaristor particles (about 40%) was chosen to be well beyond the percolation threshold.

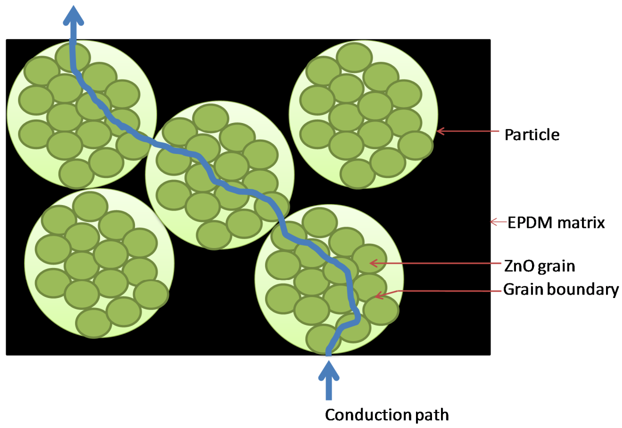

Fig. 1: Schematic of composite materials

Close and Return

Experimental setup
The current-voltage curves were measured using a 6.5 kV FUG generator (50 mA) with the LabView interface for automatic acquisition. Schematic of volume resistivity measurements is shown in Fig. 2. Aluminum plates 50 mm diameter served as electrodes. The cell was placed in an oven heated to 20℃, 40℃, 60℃ or 80℃ in order to check the electronic transport behaviour.

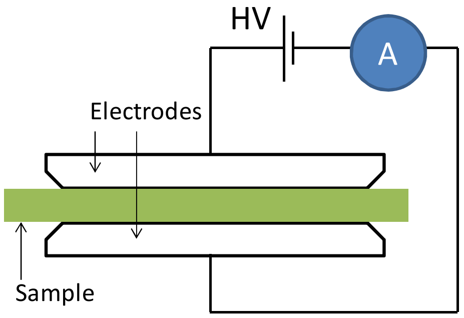

Fig. 2: Schematic of electrode configuration

The current is measured continuously while the voltage is increasing from 0 to 1300 Volt.

IV. RESULTS

The current density, obtained by dividing the measured current by the electrode surface, is plotted against voltage (Fig. 3) in linear scale. It appears that the apparent threshold voltage decreases with increasing temperature from 20℃ to 80℃. In other words, at a given volta ge (e.g. 1200 V) the current density increases with increasing temperature. Below 400 V, the current was not measurable. To avoid thermal run away observed at 1400 V, the sample was not stressed above 1300 V. EPDM matrix and additives for mixing may act as donor or acceptor of electron. However charge carrier mobilities and concentrations are very low as the conductivity of EPDM is $\sigma_{\mathrm{EPDM}} = 10^{-15}$ S.m^{-1} [10]. Thus, conduction in the matrix can be considered negligible in the presence of parallel path microvaristors, and conduction mechanism can be treated as that of a percolated diode network.

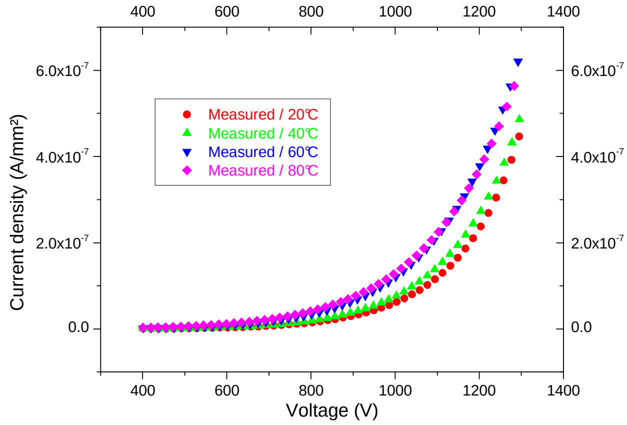

Fig. 3: (Linear scale) Experimental data of current density

V. ANALYSIS AND MODEL FITTING

In order to extract quantitative data from the measurements, the Shockley equation (Eq. 3) was used. The results of fitting are presented in Fig. 4. The fitting parameters MI_S and N are shown in Table 1.

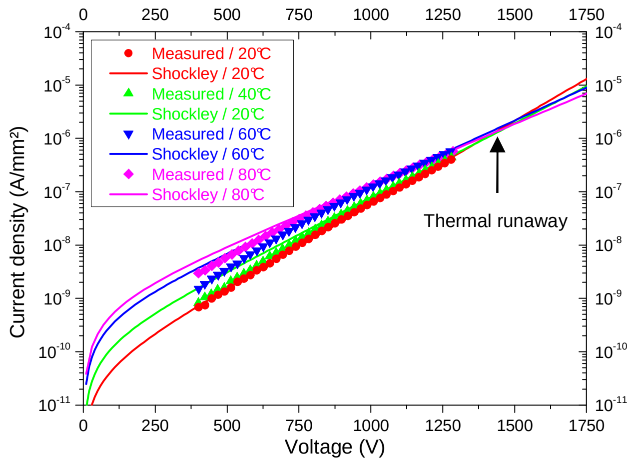

Fig. 4: (Logarithmic scale) Comparison between experimental data (Symbols) of current density and analytical fit (Continuous lines) using Eq. [3]

The number of averaged series activated diodes N - increases from 5840 to 6263 with increasing temperature from 20℃ to 80℃. Knowing the grain size of ZnO (~ 4 µm), we obtained an averaged conduction path length from one electrode to another ranging from 23.4 mm to 25 mm for 20℃ to 80℃.

A striking observation was the convergence of analytical current density curves at around 1400 V (Fig. 4), which corresponds to the experimental thermal breakdown at 20℃. In terms of energy balance, this regime corresponds to a dissipated electrical power equal to or above the thermal dissipation ability of composite.

Close and Return

Table 1 **Values obtained from analytical fitting. Two parameters were extracted: *N* and *MIs*.**

T (°C)	T (K)	1/T (K-1)	Number of diodes *N*	Grain size (µm)	R^2	$MIs/T^{4.5}$	Conduction path length (mm)
20	293.15	0.00341	5840	4	0.99993	1.4E-07	23.4
40	313.15	0.00319	5866	4	0.99982	2.7E-07	23.5
60	333.15	0.003	6117	4	0.99948	7.9E-07	24.5
80	353.15	0.00283	6263	4	0.99964	1.3E-06	25

Plotting $MI_S/T^{4.5}$ versus 1/T (Fig. 5), it is possible to assess the gap energy E_g.

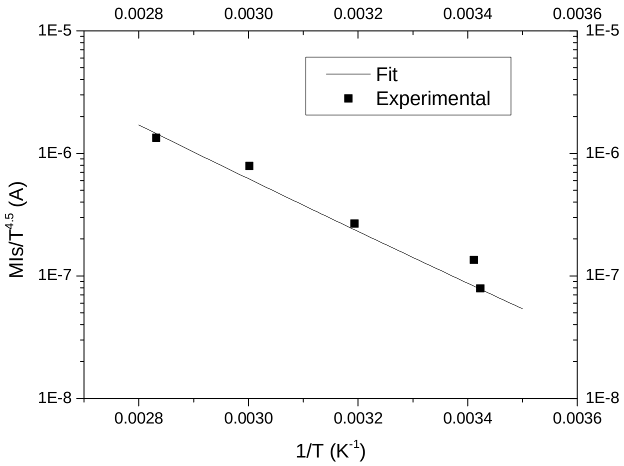

Fig. 5: The Arrhenius plot of *MIs*/T$^{4.5}$ versus 1/*T*

MI_{0S} was found to be equal at 1.10^{-13} A/K$^{4.5}$. The term $-E_g/k$ in the exponential is equal at -3500 K. Therefore, the gap energy E_g is equal at 0.3 eV. This value is in agreement with literature [6]. A missing value is the number of M in-parallel connected diodes which is contained in the pre-factor of Eq. [3]. Complementary experiments including different area surface measurements would be required to address this issue.

CONCLUSIONS

In summary, we have shown a technique for characterizing electrical properties of a varistor composite. Using current-voltage curves at different temperatures, we determined gap energy which is in agreement with reported results in literature. The thermal analysis showed an unexpected result which is the indirect consequence of thermal breakdown. The intrinsic value of varistor composite and their dependency on temperature and electric field allow modeling of the behavior of such materials in HVDC accessories and checking their efficiency in controlling the field distribution.

Acknowledgments

We acknowledge Mark Rikel for material analysis, Ludovic Boyer, Nabila Zebouchi and Christelle Mazel for materials supply, and all of them including Christian Frohne for fruitful discussions.

REFERENCES

[1] A. Janotti and C. G. Van de Walle, "Fundamentals of zinc oxide as a semiconductor," *Reports on Progress in Physics*, vol. 72, no. 12, p. 126501, Dec. 2009.

[2] U. Ozgur, Y. I. Alivov, C. Liu, A. Teke, M. a. Reshchikov, S. Dogan, V. Avrutin, S.-J. Cho, and H. Morkoc, "A comprehensive review of ZnO materials and devices," *Journal of Applied Physics*, vol. 98, no. 4, p. 041301, 2005.

[3] E. Jonsson and L. Palmovist, "A Field Grading Material," *PATENT*, pp. 1–12, 2007.

[4] M. a. Alim, S. Li, F. Liu, and P. Cheng, "Electrical barriers in the ZnO varistor grain boundaries," *Physica Status Solidi (a)*, vol. 203, no. 2, pp. 410–427, Feb. 2006.

[5] H. Bong, W. H. Lee, D. Y. Lee, B. J. Kim, J. H. Cho, and K. Cho, "High-mobility low-temperature ZnO transistors with low-voltage operation," *Applied Physics Letters*, vol. 96, no. 19, p. 192115, 2010.

[6] P. Cheng, S. Li, L. Zhang, and J. Li, "Characterization of intrinsic donor defects in ZnO ceramics by dielectric spectroscopy," *Applied Physics Letters*, vol. 93, no. 1, p. 012902, 2008.

[7] L. Donzel, F. Greuter, and T. Christen, "Nonlinear resistive electric field grading part 2: Materials and Applications," *IEEE Electrical Insulation Magazine*, vol. 27, pp. 18–29, 2011.

[8] X. Wang, S. Herth, T. Hugener, R. W. Siegel, J. K. Nelson, L. S. Schadler, H. Hillborg, and T. Auletta, "Nonlinear Electrical Behavior of Treated ZnO-EPDM Nanocomposites," *2006 IEEE Conference on Electrical Insulation and Dielectric Phenomena*, pp. 421–424, Oct. 2006.

[9] S. M. Sze and K. K. Ng, *Physics of semiconductor devices*, Wiley. 2007, pp. 90–102.

[10] E. Martensson and U. Gafvert, "A three-dimensional network model describing a non-linear composite material," *Journal of Physics D: Applied Physics*, vol. 37, no. 1, pp. 112–119, Jan. 2004.

Close and Return

GLOSSARY

PDF: Portable Document Format
RTF: Rich Text Format